



## Characterization of smearing patterns in ball nose end milling process

**Biondani, F.; Bissacco, G.; Hansen, H. N.**

*Publication date:*  
2017

*Document Version*  
Publisher's PDF, also known as Version of record

[Link back to DTU Orbit](#)

*Citation (APA):*  
Biondani, F., Bissacco, G., & Hansen, H. N. (2017). *Characterization of smearing patterns in ball nose end milling process*. Abstract from euspen's 17th International Conference & Exhibition, Hannover, Germany.

---

### General rights

Copyright and moral rights for the publications made accessible in the public portal are retained by the authors and/or other copyright owners and it is a condition of accessing publications that users recognise and abide by the legal requirements associated with these rights.

- Users may download and print one copy of any publication from the public portal for the purpose of private study or research.
- You may not further distribute the material or use it for any profit-making activity or commercial gain
- You may freely distribute the URL identifying the publication in the public portal

If you believe that this document breaches copyright please contact us providing details, and we will remove access to the work immediately and investigate your claim.

## Characterization of smearing patterns in ball nose end milling process.

F. Biondani<sup>1</sup>, G. Bissacco<sup>1</sup>, H. N. Hansen<sup>1</sup>

<sup>1</sup>Department of Mechanical Engineering, Technical University of Denmark

[frgbio@mek.dtu.dk](mailto:frgbio@mek.dtu.dk)

### Abstract

Very shallow depth of cut are used in ball end milling finishing operation in order to minimize the chip thickness, therefore reducing the surface roughness. When the chip dimension reaches a certain thickness threshold (the minimum uncut chip thickness), the cutting dynamic switches from effective material removal to ploughing and smearing. Smearing effects can significantly enhance the surface roughness. Another important factor is the choice of the appropriate tool path, which strongly affect the tool engagement condition and surface roughness. In this work, smearing pattern produced on mould steel by cBN ball end mill, are characterized by means of SEM analysis. The results show that the location of the smearing pattern is strictly connected with the relative direction of cutting speed and feed and step over direction. Furthermore, a comparison with the theoretical chip thickness distribution confirms that the smearing of the material occurs in the area in which the chip thickness approaches to zero.

Machining, smearing, surface topology

### 1. Introduction

The Interaction between tool and workpiece determines the topology of the generated surface and, in turn, the resulting roughness. Low surface roughness is required in several applications such as mould manufacturing industry. In order to target this need a low depth of cut is used while machining for finishing operations. The cutting edge radius of the ball end mill plays a key role in this. While it can be considered infinitely sharp in a roughing operation, the dullness of the cutting edge must be considered when the chip thickness is reduced more and more [1]. Once a certain local thickness is reached, called minimum uncut chip thickness (MUCT) [2], the tool is not able to remove material, that is therefore deformed and smeared over the surface [3]. In this work, smearing patterns produced by machining steel surfaces using a ball end mill were characterized by means of SEM analysis. The tool engagement conditions were varied and the developed smearing pattern is discussed.

### 2. Experimental work

The test part consists in a steel flat surface with approximately 52-54 HRC hardness. The surface was machined using a cBN ball end mill with two flutes and a ball radius of 0.5 mm. The machining strategy, in terms of tool path and cutting parameters, were varied during the tests, Figure 1. In this way it is possible to observe and characterize the surface topology produced in different cutting configurations. The four tool paths studied in this work are represented in Figure 1 and here called tool path A, B, C and D. Every configuration has a different relative orientation with respect to the cutting velocity, feed direction and step over direction. Several tracks were produced over the surface of the test part maintaining an inclination of 40° between the tool and workpiece to avoid the zero cutting speed part of the tool edge. Two sets of cutting parameters were used: depth of cut, step over, feed per tooth and rotational speed were respectively 15 µm, 50 µm, 15 µm and 13000 RPM for the

first set and 25 µm, 100 µm, 25 µm and 1300 RPM for the second set. Surfaces were characterized by means of SEM analysis.

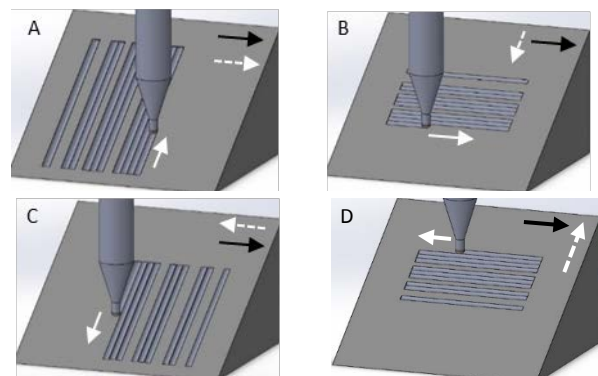


**Figure 1.** Different tool paths. The white solid arrow indicates the feed direction, the dashed white arrow the step over while the black arrow the cutting speed direction.

### 3. SEM characterization

Similar smearing patterns are observed for both sets of cutting parameters, even though for the second set the smearing phenomena is more evident. In tool path A (Figure 2 left), the cutting speed matches the step over direction. The feed marks left by the teeth are clearly visible and a clean cut separates every tool pass. At the end of the cutting edge engagement a wave-like structure is visible protruding in the opposite direction to the feed. In tool path C (Figure 2 right), the direction of the cutting speed is the opposite of the step over direction. The wave-like structures are still visible but material is piled up between subsequent tool passages.

In tool path B and D (Figure 3 left and right), the cutting speed is now parallel to the feed direction, concordant in B and discordant in D. Piling up of material is present in D where the cutting speed points toward the freshly generated surface, while the wave-like structures are localized along two subsequent tool passes in both cases.

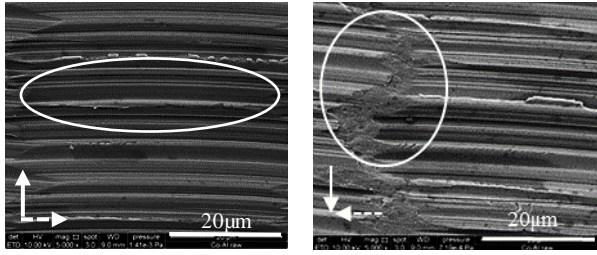


**Figure 2.** Surface generated by tool path A (left) and C (right). Arrows show the directions of step over (dashed white) and feed (solid white). The ironing process and wave like structure are highlighted by a circle.

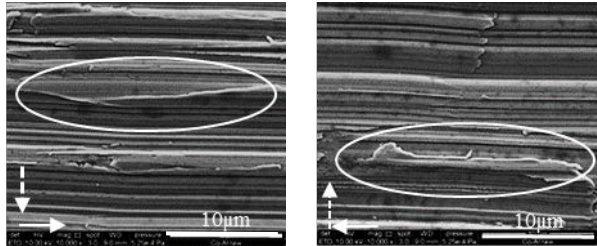


**Figure 3.** Surface generated by tool path B (left) and D (right). Arrows show the directions of step over (dashed white) and feed (solid white). The wave like structures are highlighted by a circle.

#### 4. Chip orientation and smearing

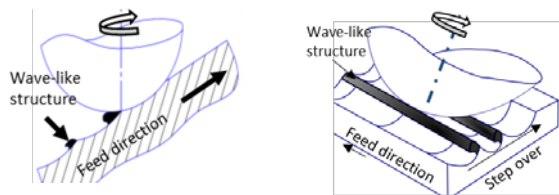


**Figure 4.** Schematic representation of the position of the side flow in tool path A and C on the left and in tool path B and D on the right

The diverse surface topologies in the four areas are ascribed to differences in the relative direction of the cutting speed and the position of the freshly machined surface. Two different kind of deformation patterns can be identified consisting in material side flow and material ironing. Differently from burrs, which are generated on the edges of the workpiece, those smearing structures are deformed over the surface and they are strongly attached to it. The position in which the material ironing occurs is connected with the cutting speed direction and it is visible only when the cutting speed points toward the freshly machined surface. In this case, the cutting edge enters the chip from the thicker side and proceeds toward the thinner side. Due to the finite size of the cutting edge radius the condition of minimum uncut chip thickness is reached close to the end of the engagement arc. At this point, the tool cannot properly remove material that is pushed and deformed in an ironing process over the already machined surface. Thus, the deformed material is visible on the surface as a small step, often showing a fracture-like surface where the cutting edge exits from the material, Figure 5 left. When the cutting velocity points in the opposite direction, i.e. the cutting edge is entering the chip from the thin side, the MUCT condition is already met. The tool may struggle in entering but, once the edge properly engages the material, a clean cut is produced. The side flow is present in every configurations and it is linked with the chip position in relation with the already machined surface, Figure 4. When the local uncut chip thickness goes below the MUCT, the thrust force becomes very high compared to the cutting force [3]. The

squeezed material flows orthogonally to the cutting speed direction where the deformation is easier because of the missing material. This generates a characteristic side flow visible as protruding wave-like structures on the surface, Figure 5 right. The theoretical local chip thickness is quantitatively shown in Figure 6. It can be noticed that the smearing phenomena are always localized where the chip thickness decreases.

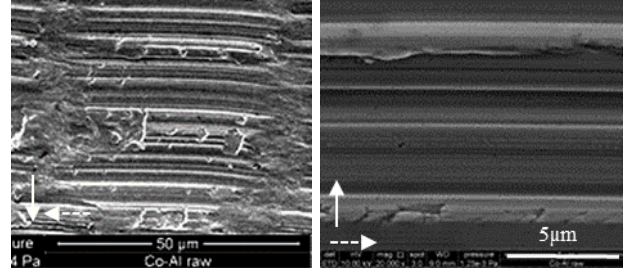


**Figure 5.** Left: material ironing produced in tool path D. Right: wave-like structure produced in tool path A. The directions of step over (dashed white) and feed (solid white) are shown by arrows.

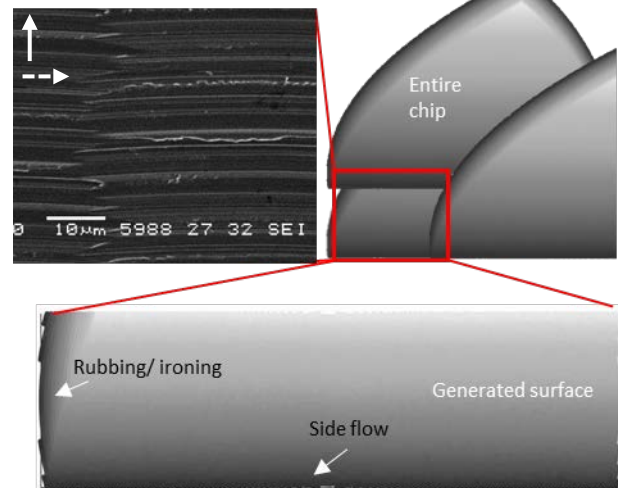


**Figure 5.** Top Left: clean cut produced by the tool entering the chip from the thin side. Top right: overall chip generated by every single tooth. Bottom: visible part of the generated surface. The grey scale, from black to light grey, indicates increasing in local chip thickness. The directions of step over (dashed white) and feed (solid white) are shown by arrows. The cutting speed points in the same direction of the step over

#### 5. Conclusion

Two different smearing phenomena occur in ball end milling where the chip thickness decreases below the MUCT: side flow and ironing. The tool path influences the relative direction of cutting velocity, feed direction and step over direction that, in turn, determines where the smearing will occur. Knowledge of the development and position of the smearing pattern can help in the selection of optimal cutting parameters and in modelling the surface generation process.

#### References

- [1] G. Bissacco, H. N. Hansen, and J. Slunsky, "Modelling the cutting edge radius size effect for force prediction in micro milling," *CIRP Ann. - Manuf. Technol.*, vol. 57, pp. 113–116, 2008.
- [2] Z. Liu, Z. Shi, and Y. Wan, "Definition and determination of the minimum uncut chip thickness of microcutting," *Int. J. Adv. Manuf. Technol.*, vol. 69, no. 5–8, pp. 1219–1232, 2013.
- [3] G. Bissacco, H. N. Hansen, and L. De Chiffre, "Size Effects on Surface Generation in Micro Milling of Hardened Tool Steel," *CIRP Ann. - Manuf. Technol.*, vol. 55, no. 2, pp. 3–6, 2006.